

Calculation of the $\eta \rightarrow \pi\pi\gamma$ Decay Rate with Finite Dispersion Relations

B.-L. Young and K. E. Lassila

National Accelerator Laboratory, Batavia, Illinois 60510*

and Department of Physics and Ames Laboratory, Iowa State University, Ames, Iowa 50010

(Received 24 October 1972)

Finite-dispersion-relation techniques as developed by Aviv and Nussinov are employed to calculate the decay rate for $\eta \rightarrow \pi^+\pi^-\gamma$ in an essentially parameter-free manner. The amplitude for this decay is obtained by crossing from the scattering process $\eta\pi \rightarrow \pi\gamma$ which has the A_2 resonance in the s and u channels and the ρ trajectory in the t channel. A single Breit-Wigner resonance of width 85 MeV for the A_2 meson directly leads to a prediction for the rate and photon momentum distribution in good agreement with experimental measurements. The so-called broad-narrow model can give agreement if couplings of each component to $\eta\pi$ and $\pi\gamma$ are properly chosen, but all pictures of the A_2 with two narrow components give inadequate results.

I. INTRODUCTION

High-energy scattering techniques and ideas incorporating duality have led to useful insight and to successful predictions for several low-energy decay-type processes. For example, the results of octet dominance in hyperon S -wave decays have been obtained without use of current algebra through incorporation of the absence-of-exotic-states requirements of duality by Nussinov and Rosner¹ and by Kawarabayashi and Kitakado.²

More recently, Aviv and Nussinov³ made a very interesting proposal which they called the finite dispersion relation (FDR) to treat three-particle decay processes; they applied this method, in particular, to $\omega \rightarrow \pi\pi\gamma$. In this approach, a fixed- t dispersion relation of finite contour radius is written for a given amplitude of the process. The low-mass resonances, i.e., the nearby poles, contributing to the s and u channels are included as usual; the high-mass contributions, i.e., the distant poles, are represented by the t -channel Regge poles according to duality arguments. In the physical region of a decay process, the high-mass contributions also exhibit the pole structure of the t channel which is usually present in a pole model, e.g., the Gell-Mann-Sharp-Wagner model.⁴ Furthermore, in the present work the residue functions of the Regge amplitudes are related to the low-energy resonance amplitude by means of finite-energy sum rules (FESR).⁵ The advantages of FDR over the conventional pole model can be summarized as follows: (a) It avoids problems with subtractions. (b) The inclusion of the t channel through duality and t -channel couplings determined by means of FESR avoids the intriguing problem of double counting which may be present in the pole model in which poles in all channels are included independently. (c) The t -

channel structure is more complete.

As a result of their investigations with the FDR approach, Aviv and Nussinov found an enhancement in the rate $\Gamma_{\omega \rightarrow \pi\pi\gamma}$ of a factor 5 over previous calculations, in agreement with the experimental bounds. This method was also applied by Gounaris and Verganelakis⁶ to $\eta \rightarrow \pi\gamma\gamma$; they found tremendous enhancement, a factor ~ 90 over the pole-dominance model. The pole-dominance model gives $\Gamma_{\eta \rightarrow \pi\gamma\gamma} \simeq 0.6$ eV, the FDR result is 70 ± 30 eV,⁶ and the experimental value is 81 ± 32 eV.⁷ From this we see that the pole-dominance model grossly underestimates this particular decay rate, and, since the FDR method gives reasonable results, the $\eta \rightarrow \pi\gamma\gamma$ calculation serves to test the soundness of the ideas behind FDR.

In fact, tests of the ideas behind FDR have not been restricted to the decay processes described above; it has been applied to scattering processes in the medium-energy range, as suggested by Barger and Phillips⁸ and carefully tested by Baacke and Engels.⁹ These authors⁹ found that the elastic πp $I_t = 0$ amplitudes so calculated are in good agreement with the results of phase-shift analysis. Further, applications to current-algebra sum rules have been carried out recently by Ellis and Weisz and by Gounaris¹⁰ with satisfactory results.

In the present work, we shall apply FDR to the decay $\eta \rightarrow \pi\pi\gamma$, which is related to the "scattering" process $\eta\pi \rightarrow \pi\gamma$ by crossing. The pole structure of the amplitude for this process is very simple in all three (s, t, u) channels, and the existing experimental decay width is quite accurate.⁷ We shall demonstrate that the FDR approach can again give good predictions, and also we are led to information about the A_2 meson and models for explaining the splitting, which has not been readily available in the past from the experimental mass

distributions.

Consideration of the pole structure for $\eta\pi \rightarrow \gamma\pi$ shows that the A_2 meson contributes in the s and u channels, and the ρ meson in the t channel. However, it is necessary to study how one should treat the A_2 meson in FESR calculations of meson-meson scattering in the context of the narrow-resonance limit. Since numerous models have been suggested to explain experiments with A_2 mass structure (or lack of it), it is of considerable interest to see what these models predict for the A_2 contribution in $\eta \rightarrow \pi\pi\gamma$, according to the FDR method. This process provides, in principle, an independent method for studying what the A_2 is made of and, *a priori*, the various A_2 models might well produce considerably different predictions for $\Gamma_{\eta \rightarrow \pi\pi\gamma}$.

In Sec. II we employ the FDR method to derive the decay amplitude for $\eta \rightarrow \pi\pi\gamma$. In Sec. III, the A_2 contribution is treated in depth for the purpose of seeing what can be learned regarding the split or nonsplit status of this elusive meson and to calculate contributions as predicted by the various A_2 descriptions appearing in the literature and tabulations. The pictures found to be discriminated against are those in which the A_2 has two narrow states of the same internal quantum numbers, the so-called high-low model, or two different spin-parity states, as found in certain experiments¹¹ or, e.g., in four-dimensional generalizations of the harmonic-oscillator quark model.¹² In Sec. IV, we discuss another criterion for the choice of the radius of the contour of FDR and demonstrate that the prescription given by Aviv and Nussinov³ indeed satisfies this criterion. We further investigate the sensitivity of our answer – for the rate of $\eta \rightarrow \pi\pi\gamma$ to changes in the contour radius – to variations due to possible Regge form factors and changes in the actual forms of the Regge trajectories. Final conclusions and further discussion are reserved till Sec. V.

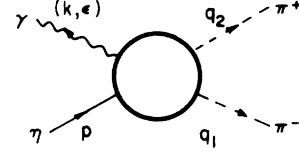


FIG. 1. Diagram for $\eta \rightarrow \pi\pi\gamma$ with four-momentum and polarization vectors labeling particle lines.

II. THE $\eta \rightarrow \pi\pi\gamma$ AMPLITUDE WITH FINITE DISPERSION RELATIONS

It should be noted first that the process $\eta \rightarrow \pi\pi\gamma$ does not have a bremsstrahlung diagram. Therefore, the amplitude which we consider for $\eta \rightarrow \pi\pi\gamma$ is as illustrated diagrammatically in Fig. 1. In Fig. 1 the 4-momenta and polarizations label the outgoing and incoming particles. The amplitude for this process is

$$A = (\epsilon^\mu) \epsilon_{\mu\nu\lambda\rho} q_1^\nu q_2^\lambda k^\rho B(\nu, t), \quad (1)$$

where the Mandelstam variables are defined as

$$\begin{aligned} s &= (p - q_1)^2 \\ &= (k + q_2)^2, \\ t &= (p - k)^2 \\ &= (q_1 + q_2)^2, \\ u &= (p - q_2)^2 \\ &= (k + q_1)^2, \end{aligned}$$

with

$$\nu = \frac{1}{2}(s - u).$$

Under $s \rightarrow u$ ($\nu \rightarrow -\nu$) crossing $B(\nu, t) = B(-\nu, t)$.

At low energies (say, ≤ 2 GeV), the internal quantum numbers of the external particles are such that only the A_2 contributes in the s and u channels. The relevant resonance amplitude can be written as

$$B_{\text{res}}(\nu, t) = -4g_{A_2\pi\gamma} g_{A_2\eta\pi} \left[\frac{t - u - m_\pi^2(m_\eta^2 - m_\pi^2)m_{A_2}^{-2}}{s - m_{A_2}^2} + \frac{t - s - m_\pi^2(m_\eta^2 - m_\pi^2)m_{A_2}^{-2}}{u - m_{A_2}^2} \right], \quad (2)$$

where $g_{A_2\pi\gamma}$ and $g_{A_2\eta\pi}$ are the physical coupling constants for $A_2\pi\gamma$ and $A_2\eta\pi$, respectively, when the A_2 is on its mass shell. These couplings are defined such that the decay amplitudes for $A_2 \rightarrow \pi\gamma$ and $A_2 \rightarrow \eta\pi$ are given, respectively, by

$$T_{A_2 \rightarrow \gamma\pi} = g_{A_2\pi\gamma} \epsilon^\mu(k) h^{\nu\lambda}(K) [(k - q)_\nu \epsilon_{\mu\lambda\sigma\tau} k^\sigma q^\tau + (k - q)_\lambda \epsilon_{\mu\nu\sigma\tau} k^\sigma q^\tau]$$

and

$$T_{A_2 \rightarrow \eta\pi} = g_{A_2\eta\pi} h^{\mu\nu}(K) (k - q)_\mu (k - q)_\nu,$$

where K and q are the 4-momenta of the A_2 and π , respectively, $h^{\mu\nu}(K)$ is the polarization tensor of the A_2 , and k is the 4-momentum of the γ or the η , depending on the process.

The ρ trajectory gives the only known contribution (excluding small contributions from daughters, which

are assumed ignorable in the literature) in the t channel where $\gamma\eta \rightarrow \pi^+\pi^-$. This is described by the amplitude for odd-signature ρ -Regge-pole exchange

$$B_{\text{Regge}}(\nu, t) = \frac{\pi\beta}{\Gamma(\alpha_\rho(t)) \sin\pi\alpha_\rho(t)} [\nu^{\alpha_\rho(t)-1} + (-\nu)^{\alpha_\rho(t)-1}], \quad (3)$$

where $\Gamma(\alpha_\rho(t))$ is used to eliminate ghost states when $\alpha_\rho(t)$ goes through negative integers and also contains a nonsense-wrong-signature zero (NWSZ). We may assume that β is weakly dependent on t , at least for t small, and take it as constant for simplicity.¹³ (See Sec. IV for further discussion. Taking out the NWSZ does not affect our conclusions.)

Following Ref. 3, we write a fixed- t dispersion integral of finite contour of radius N :

$$B(\nu, t) = \frac{1}{2\pi i} \oint \frac{B(\nu', t)}{\nu' - \nu} d\nu' \equiv B_L(\nu, t) + B_H(\nu, t), \quad (4)$$

where

$$B_L(\nu, t) \equiv \frac{1}{\pi} \int_0^N \frac{2\nu' \text{Im}B(\nu', t)}{\nu'^2 - \nu^2} d\nu' \quad (5)$$

and

$$B_H(\nu, t) \equiv \frac{1}{2\pi i} \int_{C_N} \frac{\nu B(\nu', t)}{\nu'^2 - \nu^2} d\nu', \quad (6)$$

where N is large enough such that the Regge representation for $B(\nu, t)$ is valid for $\nu \gtrsim N$; C_N is a circle of radius N centered at $\nu = 0$.

Substituting Eq. (2) and Eq. (3) into Eq. (5) and Eq. (6), respectively, we obtain

$$B_L(\nu, t) = -4g_{A_2\pi\gamma} g_{A_2\eta\pi} \left[\frac{2t + m_{A_2}^2 - m_\eta^2 - 2m_\pi^2 - m_\pi^2(m_\eta^2 - m_\pi^2)m_{A_2}^{-2}}{\nu - (m_{A_2}^2 - \frac{1}{2}m_\eta^2 - m_\pi^2 + \frac{1}{2}t)} + (\nu \rightarrow -\nu) \right] \quad (7)$$

from the resonance contribution, and

$$B_H(\nu, t) = -2 \frac{\beta}{\Gamma(\alpha_\rho(t))} \sum_{n=0}^{\infty} \left(\frac{\nu}{N}\right)^{2n} \frac{N^{\alpha_\rho(t)-1}}{\alpha_\rho(t) - 2n - 1} \quad (8)$$

from the Regge amplitude. The Regge coupling β is determined from the resonance coupling by means of the FESR. The lowest-moment sum rule

$$\frac{\beta}{\Gamma(\alpha_\rho(t))} \frac{N^{\alpha_\rho(t)+1}}{\alpha_\rho(t)+1} = \frac{1}{\pi} \int_0^N d\nu \nu \text{Im}B(\nu, t) \quad (9)$$

is used to obtain the Regge residue at $t=0$,¹³

$$\beta = 6\sqrt{\pi} N_0^{-3/2} g_{A_2\pi\gamma} g_{A_2\eta\pi} (m_{A_2}^2 - \frac{1}{2}m_\eta^2 - m_\pi^2) \times [m_{A_2}^2 - m_\eta^2 - 2m_\pi^2 - m_\pi^2(m_\eta^2 - m_\pi^2)m_{A_2}^{-2}], \quad (10)$$

where $N = N_0 + \frac{1}{2}t$, and the ρ trajectory is taken as

$$\alpha_\rho(t) = \frac{1}{2} + t/2m_\rho^2. \quad (11)$$

It may be noted that the same N is used as the "cutoff" in the FESR as in the FDR, except that in the former $t=0$ explicitly.

The approach of Aviv and Nussinov³ is followed in choosing the cutoff, or the radius of the circular contour in the FDR, N (or N_0), as the average value of $M_{A_2}^2$ and $M_{A_2'}^2$, where A_2' is the Regge recurrence of the A_2 . With the A_2 trajectory as

$$\alpha_{A_2}(t) = \frac{1}{2} + 3t/2m_{A_2}^2, \quad (12)$$

this recurrence occurs at

$$m_{A_2'}^2 = \frac{7}{3}m_{A_2}^2.$$

This leads to

$$N_0 = \frac{5}{3}m_{A_2}^2 - \frac{1}{2}m_\eta^2 - m_\pi^2 = 2.65 \text{ GeV}^2. \quad (13)$$

From Eqs. (4)–(13) one sees that the decay amplitude will be completely determined if $g_{A_2\pi\gamma}$ and $g_{A_2\eta\pi}$ are determined. A further justification for choosing (13) will be discussed in Sec. IV.

To conclude this section, let us note that Eq. (4) can be obtained in the conventional way with the contour closed at infinity:

$$B_H(\nu, t) = \frac{1}{\pi} \int_N^\infty \frac{2\nu' \text{Im}B(\nu', t)}{\nu'^2 - \nu^2} d\nu',$$

with $\text{Im}B(\nu, t) = \text{Im}B_{\text{Regge}}(\nu, t)$ substituted in the above expression. This is no more than a statement of local duality. In the case where an amplitude needs a subtraction, FDR enables one to determine the subtraction constant.

III. THE A_2 -MESON CONTRIBUTION AND DETERMINATION OF $g_{A_2 \pi \gamma}$ and $g_{A_2 \eta \pi}$

The couplings of $g_{A_2 \pi \gamma}$ and $g_{A_2 \eta \pi}$ appearing in Eq. (7) are the physical coupling constants and are determined from the decay widths of $A_2 \rightarrow \pi \gamma$ and $A_2 \rightarrow \pi \eta$, respectively. Since the A_2 might not be a conventional resonance, we shall investigate in more detail its role when it contributes to the direct channel, especially in the narrow-resonance limit as applied in FESR. In the present case, since the contributions of the A_2 come from the tail of the resonance where s and $u \leq (m_\eta - m_\pi)^2$, the narrow-resonance limit is indeed justified. There exists direct experimental evidence on $A_2 \rightarrow \pi \eta$, but not on $A_2 \rightarrow \pi \gamma$. We shall use the vector-meson-dominance model to calculate the latter from the decay $A_2 \rightarrow \pi \rho$.

A. Calculation with the A_2 as a Single Meson

The results obtained at CERN¹⁴ showing two-peaked structure for the A_2 meson in $\pi^- \rho$ collisions at 7.0 GeV/c pion momentum were placed in considerable doubt when the Northeastern University-State University of New York at Stony Brook collaboration¹⁵ could not confirm the split-peak structure in a similar experiment under conditions nearly duplicating those of the CERN missing-mass groups. The need for a third experiment has been mentioned,¹⁶ since the latter effort was done with somewhat poorer resolution than CERN's, but such a third experiment was suggested not worth the cost unless resolution can be improved over both earlier experiments.

Assuming that the A_2 consists of a single conventional resonance, we take the mass $M_{A_2} \simeq 1300$ MeV, and the width $\Gamma_{A_2} = 85$ MeV. The fractional decays into $\rho\pi$ and $\eta\pi$ are given in Ref. 7 as 76% and 18%, respectively. A fit using SU(3) relations reported in Ref. 17 found similar numbers. In comparing these values with past best branching fractions, one sees that in approximately one year the $\rho\pi$ branching ratio has been reduced and the $\eta\pi$ fraction increased significantly. The main reason for this change is the large branching ratio found by a Berkeley group for $A_2^+ \rightarrow \eta\pi^+$.¹⁸ (If the A_2^- is actually unsplit, as suggested by Ref. 15, then the difference in charge state has no significance.)

With the branching ratios of Ref. 7, the coupling constants are calculated as

$$\begin{aligned} g_{A_2^{\pm} \rho^0 \pi^{\mp}} / 4\pi &= 1.79 \text{ GeV}^{-4}, \\ g_{A_2^{\pm} \eta \pi^{\mp}} / 4\pi &= 0.619 \text{ GeV}^{-2}. \end{aligned} \quad (14a)$$

These follow from the expressions for $T_{A_2 \rightarrow \pi \eta}$ and $T_{A_2 \rightarrow \pi \gamma}$ given after Eq. (2), which are used to calculate the decay widths,

$$\begin{aligned} \Gamma_{A_2^{\pm} \rightarrow \rho^0 \pi^{\pm}} &= \frac{1}{20} \frac{1}{4\pi} g_{A_2^{\pm} \rho^0 \pi^{\mp}}^2 [\lambda(m_{A_2}^2, m_\rho^2, m_\pi^2)]^5 m_{A_2}^{-5}, \\ \Gamma_{A_2^{\pm} \rightarrow \gamma \pi^{\pm}} &= \frac{1}{20} \frac{1}{4\pi} g_{A_2^{\pm} \gamma \pi^{\mp}}^2 [\lambda(m_{A_2}^2, m_\pi^2, 0)]^5 m_{A_2}^{-5}, \\ \Gamma_{A_2^{\pm} \rightarrow \eta \pi^{\pm}} &= \frac{1}{30} \frac{1}{4\pi} g_{A_2^{\pm} \eta \pi^{\mp}}^2 [\lambda(m_{A_2}^2, m_\eta^2, m_\pi^2)]^5 m_{A_2}^{-7}, \end{aligned}$$

where

$$[\lambda(x, y, z)]^2 = x^2 + y^2 + z^2 - 2xy - 2yz - 2zx.$$

Either the ρ decay width or the results of recent ω - ρ interference experiments¹⁹ leads to a ρ - γ coupling constant ef_ρ^{-1} given by

$$f_\rho^2 / 4\pi = 2.56 \pm 0.22.$$

Then

$$\begin{aligned} g_{A_2^{\pm} \pi^{\mp} \gamma}^2 / 4\pi &= \alpha (g_{A_2^{\pm} \rho^0 \pi^{\mp}}^2 / 4\pi) (f_\rho^2 / 4\pi)^{-1} \\ &\cong 5.1 \times 10^{-3} \text{ GeV}^{-4}, \end{aligned} \quad (14b)$$

which gives

$$\Gamma_{A_2^{\pm} \rightarrow \pi^{\pm} \gamma} = 0.9 \text{ MeV},$$

or a branching ratio of 1% for the $\pi\gamma$ mode.²⁰ These numbers, Eqs. (14a) and (14b), when substituted into Eq. (4) lead to²¹

$$\Gamma_{\eta \rightarrow \pi \pi \gamma} = 0.148 \text{ keV}, \quad (15)$$

when an error of perhaps 20% should be included due to the uncertainties in the A_2 partial widths.²² This compares favorably with the experimental average value⁷

$$\Gamma_{\eta \rightarrow \pi \pi \gamma}^{\text{exp}} = 0.123 \pm 0.028 \text{ keV}. \quad (16)$$

In Fig. 2, we plot the photon energy distribution obtained in our model. The experimental data are taken from Cnops *et al.*²³ The solid curve labeled FDR is the result given by the present FDR calculation; the dashed line gives the purely phase-space prediction. Clearly the solid curve gives a very good fit to the data, improving considerably on the dashed curve at high p_γ values. The curve can be calculated absolutely, but the data are given in relative intensity units in Ref. 23, necessitating normalization to be adjustable.

The contribution of the high-energy amplitude alone to $\Gamma_{\eta \rightarrow \pi \pi \gamma}$ is 0.059 keV, and the low-energy amplitude alone gives 0.02 keV. Let us remark that it is crucial to use the low-energy form Eq. (7) in Eq. (4). If one uses the B_{res} of Eq. (2), the predicted rate would be 0.062 keV instead of Eq. (16).

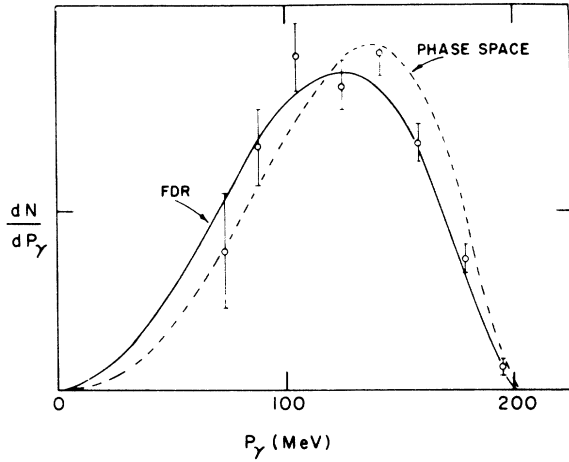


FIG. 2. Photon intensity distribution vs photon momentum in $\eta \rightarrow \pi^+ \pi^- \gamma$. The solid curve labeled FDR gives the result of the present finite-dispersion-relation calculation; the dashed curve is the result following purely from phase space. The data are from Ref. 23 and do not give an absolute normalization.

B. Prediction from the Coupled-Resonance Model of the A_2

In 1967 it was suggested^{24,25} that the $A_2(1300)$ meson contained two $J^P = 2^+$ particles which could mix to cause possible complicated mass shapes, calculable via a mass matrix approach. With this method, the amplitude for a reaction proceeding from an initial state r to some final state n through the two particle A_2 system is

$$T_{nr}(s) = F^n(s) D^{-1}(s) G^r(s), \quad (17)$$

where the decay and production vertex vectors are, respectively,

$$F^n(s) = (F_1^{(n)}, F_2^{(n)})$$

and

$$\vec{G}^r(s) = (G_1^{(r)}, G_2^{(r)}).$$

The function $D(s)$ is s minus the mass matrix, and its inverse will be parametrized as²⁵

$$D^{-1}(s) = \frac{1}{(s - s_+)(s - s_-)} \times \begin{pmatrix} s - m_2^2 + i\gamma_2 m_2 & -\xi(m_1 + m_2) \\ -\xi(m_1 + m_2) & s - m_1^2 + i\gamma_1 m_1 \end{pmatrix}, \quad (18a)$$

where the mixing element is, in general, complex, $\xi = c + id$, and

$$s_{\pm} = \frac{1}{2} \{ m_1^2 + m_2^2 - i(\gamma_1 m_1 + \gamma_2 m_2) \pm [(m_1^2 - i\gamma_1 m_1 - m_2^2 + i\gamma_2 m_2)^2 + 4\xi^2(m_1 + m_2)^2]^{1/2} \}. \quad (18b)$$

For our FDR calculation $n = (\pi\gamma)$ and $r = (\pi\eta)$, since $F_i^{(n)}$ describes the decay of meson i into the $\pi\gamma$ final state and $G_i^{(r)}$ describes its production from the $\pi\eta$ initial state.

The narrow-resonance limit of the amplitude Eq. (17) is readily found to be

$$T_{nr}(s) \rightarrow (F_1^{(n)} G_1^{(r)} + F_2^{(n)} G_2^{(r)}) (s - m_0^2 + i\epsilon)^{-1}, \quad (19)$$

where $m_0^2 = \frac{1}{2}(m_1^2 + m_2^2)$. Arguments can be made to limit the size of the off-diagonal elements in energy units by the A_2 width; this makes derivation of (19) obvious.²⁶ Equation (19) indicates a single pole in the limit, but with residue modified from that for the no-mixing single-Breit-Wigner case.

The experimental limit on $\Gamma_{\eta \rightarrow \pi\pi\gamma}$ can be directly cast into limits on the absolute value squared of the residue $F_1^{(\pi\gamma)} G_1^{(\pi\eta)} + F_2^{(\pi\gamma)} G_2^{(\pi\eta)}$. Let the F 's and G 's be defined so that $|F^{(\pi\gamma)} G^{(\pi\eta)}|^2 = 13.7 \text{ MeV}^2$ for the single-Breit-Wigner case written in the form of Eq. (17). Then Eq. (16), $\Gamma_{\eta \rightarrow \pi\pi\gamma} = 0.123 \pm 0.28 \text{ keV}$, implies that

$$11 \leq |F_1^{(\pi\gamma)} G_1^{(\pi\eta)} + F_2^{(\pi\gamma)} G_2^{(\pi\eta)}|^2 \leq 14 \text{ MeV}^2 \quad (20)$$

for the more general case of two mesons. For the single-Breit-Wigner A_2 resonance, F_2 and G_2 are zero and the experimental branching ratios $\Gamma_{A_2 \rightarrow \pi\rho}$ and $\Gamma_{A_2 \rightarrow \pi\eta}$ determine $|F_1^{(\pi\gamma)} G_1^{(\pi\eta)}|^2 = 13.7 \text{ MeV}^2$ as an absolute prediction within the framework of this FDR-FESR calculation. Models with a broad and a narrow component in the A_2 can readily satisfy condition (20), provided most of the coupling to the $\pi\rho$ and $\pi\eta$ is through the broad component. However, for two narrow resonances of width, say 25 MeV each (and masses 1290 and 1310 MeV given in Ref. 7), as in the high-low picture of the A_2 , it would appear that the largest $|F_1^{(\pi\gamma)} G_1^{(\pi\eta)} + F_2^{(\pi\gamma)} G_2^{(\pi\eta)}|^2$ that can be made, regardless of the assumed ratios of $\pi\rho$ and $\pi\eta$ couplings, is 5 MeV^2 , which is well below the lower limit in Eq. (20). This number of 5 MeV^2 is a model-independent upper limit for two narrow-width $J^P = 2^+$ objects (making up the A_2) based only on the total width (or coupling) available. Specific descriptions of how the heavier particle couples to $\pi\rho$ and $\pi\eta$ compared with the lighter particle will generally lead to a smaller than 5 MeV^2 value of $|F_1^{(\pi\gamma)} G_1^{(\pi\eta)} + F_2^{(\pi\gamma)} G_2^{(\pi\eta)}|^2$.

Models ascribing different J^P to the two peaks will yield a result considerably lower than 5 MeV^2 , as one of these particles does not couple to $\pi\rho$ or $\pi\eta$. Then, the largest $|F_1^{(\pi\gamma)} G_1^{(\pi\eta)} + F_2^{(\pi\gamma)} G_2^{(\pi\eta)}|^2$ can be is 1.2 MeV^2 , which follows from a width of 25 MeV for one $J^P = 2^+$ particle.

The very special case^{11,12} of a $J^{PC} = 1^{-+}$ meson

and a $J^P = 2^{++}$ meson making up the A_2 requires extra attention, because the mesons couple differently to $\pi\rho$ and $\pi\eta$. Let us denote this $J^P = 1^{-+}$ meson by \bar{A} . The couplings of \bar{A} to the $\pi\gamma$ and $\pi\eta$ systems are given by

$$T_{\bar{A}\pi\gamma} = g_{\bar{A}\pi\gamma} \epsilon^\mu(k) \epsilon_{\mu\nu\lambda\rho} \epsilon_{\bar{A}}^\nu(k) q^\lambda k^\rho$$

and

$$T_{\bar{A}\pi\eta} = g_{\bar{A}\pi\eta} \epsilon_{\bar{A}}^\mu(k) (q+k)_\mu.$$

The conventions are those appearing in the expressions below Eq. (2), except that the corresponding quantities characterizing the A_2 are changed to \bar{A} . The \bar{A} contribution to $B_{\text{res}}(\nu, t)$ is

$$B_{\text{res}}^{(\bar{A})}(\nu, t) = -g_{\bar{A}\pi\gamma} g_{\bar{A}\pi\eta} \times \left[\frac{1}{\nu - (m_{\bar{A}}^2 - \frac{1}{2}m_\eta^2 - m_\pi^2 + \frac{1}{2}t)} + (\nu \rightarrow -\nu) \right], \quad (21)$$

which is incidentally also the low-energy contribution to $B(\nu, t)$, i.e.,

$$B_L^{(\bar{A})}(\nu, t) = B_{\text{res}}^{(\bar{A})}(\nu, t). \quad (22)$$

The high-energy amplitude still has the form (8). However, the residue function is determined by both the contributions of (the narrow) A_2 and \bar{A} . The contribution from the $J^P = 2^{++}$ component of the A_2 is still of the form (10); the contribution from \bar{A} is given by

$$\beta(\bar{A}) = 3N_0^{-3/2} g_{\bar{A}\pi\gamma} g_{\bar{A}\pi\eta} (m_{\bar{A}}^2 - \frac{1}{2}m_\eta^2 - m_\pi^2). \quad (23)$$

The decay formulas for $\bar{A} \rightarrow \pi\rho$, $\pi\gamma$, and $\pi\eta$ can be calculated to be

$$\Gamma_{\bar{A}^{\pm} \rightarrow \pi^{\pm}\rho^0} = \frac{1}{24} \frac{1}{4\pi} g_{\bar{A}^{\pm}\rho^0}^2 [m_{\bar{A}} \lambda(1, m_\pi^2/m_{\bar{A}}^2, m_\rho^2/m_{\bar{A}}^2)]^3,$$

$$\Gamma_{\bar{A}^{\pm} \rightarrow \pi^{\pm}\gamma} = \frac{1}{24} \frac{1}{4\pi} g_{\bar{A}^{\pm}\gamma}^2 [m_{\bar{A}} \lambda(1, m_\pi^2/m_{\bar{A}}^2, 0)]^3,$$

$$\Gamma_{\bar{A}^{\pm} \rightarrow \pi^{\pm}\eta} = \frac{1}{12} \frac{1}{4\pi} g_{\bar{A}^{\pm}\eta}^2 [m_{\bar{A}} \lambda(1, m_\pi^2/m_{\bar{A}}^2, m_\eta^2/m_{\bar{A}}^2)]^3.$$

For definiteness, we take the masses (this leads to very little error) and widths of A_2 and \bar{A} to be the same, e.g., 1300 MeV and 25 MeV, respectively. The couplings calculated from the above formula are

$$g_{\bar{A}\rho\pi}^2/4\pi = 0.547 \chi_{\pi\rho} \text{ GeV}^{-2},$$

$$g_{\bar{A}\gamma\pi}^2/4\pi = 1.56 \times 10^{-3} \chi_{\pi\gamma} \text{ GeV}^{-2},$$

$$g_{\bar{A}\eta\pi}^2/4\pi = 0.261 \chi_{\pi\eta} \text{ GeV}^{-2},$$

where $\chi_{\pi\rho}$ and $\chi_{\pi\eta}$ are the branching ratios for these two modes of the \bar{A} decay. Since $\chi_{\pi\eta} + \chi_{\pi\rho} \leq 1$, the maximal value of $g_{\bar{A}\gamma\pi} g_{\bar{A}\eta\pi}$ is obtained for $\chi_{\pi\rho} = \chi_{\pi\eta} = \frac{1}{2}$, which leads to

$$g_{\bar{A}\gamma\pi} g_{\bar{A}\eta\pi} \leq 0.61 g_{A_2\gamma\pi} g_{A_2\eta\pi}.$$

Denoting the contributions of A_2 to the low- and high-energy amplitudes by $B_L^{(A_2)}$ and $B_H^{(A_2)}$, we have

$$B_L^{(\bar{A})} \leq 0.20 B_L^{(A_2)},$$

$$B_H^{(\bar{A})} \leq 0.22 B_H^{(A_2)}.$$

This gives the prediction

$$\Gamma_{\eta \rightarrow \pi\pi\gamma} \lesssim 0.019 \text{ keV}, \quad (24)$$

which is well below the experimental number listed in Eq. (16). Thus we feel that this model^{11,12} is also strongly ruled out as a possibility for the \bar{A}_2 (should it turn out to be split).

Still another possibility discussed in the literature is that only one of the components of the A_2 couples to the $\pi\rho$ and $\pi\eta$. It is possible to satisfy the sum rule (20), with one of the G_i and/or F_i ($i = 1, 2$) being zero, only if the nonzero coupling is to a broad state of total width about 80 MeV.

IV. DETERMINATION OF THE $\rho\eta\gamma$ COUPLING CONSTANT AND THE CUTOFF PARAMETER N_0

In this section, we shall examine the question of uniqueness of our choice of N_0 , especially in the sense of the narrow-resonance approximation. The choice of N is not a new problem in the evaluation of FESR. To put the question in perspective, we briefly review: Let us differentiate Eqs. (4) and (9) with respect to N , obtaining

$$\begin{aligned} \text{Im}B(N, t) &= \frac{\pi\beta}{\Gamma(\alpha_\rho(t))} N^{\alpha_\rho(t)-1} \\ &+ \frac{d\beta}{dN} \frac{\pi}{\Gamma(\alpha_\rho(t))} N^{\alpha_\rho(t)} \left[1 - \left(\frac{\nu}{N} \right)^2 \right] \\ &\times \sum_n \frac{(\nu/N)^{2n}}{\alpha_\rho(t) - 2n - 1} \end{aligned} \quad (25a)$$

and

$$\begin{aligned} \text{Im}B(N, t) &= \frac{\pi\beta}{\Gamma(\alpha_\rho(t))} N^{\alpha_\rho(t)-1} \\ &+ \frac{d\beta}{dN} \frac{\pi}{\Gamma(\alpha_\rho(t))} N^{\alpha_\rho(t)} \frac{1}{\alpha_\rho(t) + 1}, \end{aligned} \quad (25b)$$

respectively. The solutions of these two equations are

$$\text{Im}B(N, t) = \frac{\pi\beta}{\Gamma(\alpha_\rho(t))} N^{\alpha_\rho(t)-1}, \quad (26a)$$

$$\frac{d\beta}{dN} = 0. \quad (26b)$$

This result, Eq. (26a), is again a restatement of duality, and (26b) is obvious because the Regge

residue function cannot depend on the cutoff since the choice of its value is at our disposal.

Now let us examine the FESR, Eq. (9). There is no problem, in principle, when N is large enough and the widths of all the contributing resonances are included. In the narrow-resonance limit, however, $\text{Im}B(\nu, t)$ is just a sum of δ functions. When N varies from the right of one resonance to the left of a neighboring one, the right-hand side of Eq. (9) is a fixed value and the left-hand side of Eq. (9) varies continuously; therefore a proper choice of N is obviously necessary.

As stated in Sec. II, our choice of N is the average value of $m_{A_2}^2$ and $m_{A_2'}^2$, following Ref. 3. This prescription is not unique; there are other criteria, e.g., the choice of N can be such that when extrapolated in t to the ρ pole the amplitude has the appropriate $\rho\pi\pi$ and $\rho\eta\gamma$ coupling constants in the numerator of Eq. (8).

When $t \rightarrow m_\rho^2$, we get from Eqs. (4) and (8)

$$\lim_{t \rightarrow m_\rho^2} (t - m_\rho^2)B(\nu, t) = \lim_{t \rightarrow m_\rho^2} (t - m_\rho^2)B_H(\nu, t) = -4\beta m_\rho^2. \quad (27)$$

As $t \rightarrow m_\rho^2$, $B(\nu, t)$ can also be expressed in terms of the ρ couplings to $\pi\pi$ and $\eta\gamma$, i.e.,

$$\lim_{t \rightarrow m_\rho^2} B(\nu, t) = -\frac{2f_{\rho\eta\gamma}f_{\rho\pi\pi}/m_\pi}{t - m_\rho^2}, \quad (28)$$

where we have described the $\rho\pi\pi$ and $\rho\eta\gamma$ vertices by $f_{\rho\pi\pi}\epsilon_\rho \cdot (q_1 - q_2)$ and $(f_{\rho\eta\gamma}/m_\pi)\epsilon_{\mu\nu\lambda\rho}\epsilon_\rho^\mu\epsilon_\gamma^\nu k^\lambda p^\rho$, respectively. The factor $1/m_\pi$ is used to make $f_{\rho\eta\gamma}$ dimensionless. We have from (27) and (28)

$$f_{\rho\eta\gamma}f_{\rho\pi\pi} = 2m_\rho^2 m_\pi \beta. \quad (29)$$

Using $f_{\rho\pi\pi}^2/4\pi = 2.56 \pm 0.4$,¹⁹ we get

$$f_{\rho\eta\gamma}^2/4\pi = 0.115\alpha, \quad (30)$$

which probably should be good to 20% due to various uncertainties.

There is no experimental information on $f_{\rho\eta\gamma}$. We can make, however, an estimate using broken SU(3) relations, to compare with the prediction in Eq. (30). Consequently,

$$f_{\rho\eta\gamma} = 3^{-1/2} f_{\omega\pi\gamma} \cos\theta_\rho - 3g_1 \sin\theta_\rho, \quad (31)$$

where θ_ρ is the η - η' mixing angle estimated from the mass formula $\tan\theta_\rho = -0.19$ (Ref. 27); $f_{\omega\pi\gamma}$ is the $\omega\pi\gamma$ coupling constant (Ref. 28); g_1 is the pseudoscalar singlet- ω - γ coupling constant. The couplings g_1 and $f_{\omega\pi\gamma}$ are related,

$$g_1 = r\sqrt{2} f_{\omega\pi\gamma}/3\sqrt{3},$$

where $r=1$ is the quark-model result.²⁷ Using vector-meson dominance, we have the $\pi^0 \rightarrow 2\gamma$ and $\eta \rightarrow 2\gamma$ amplitudes

$$F_{\pi^0\gamma\gamma} = (2e/3f_\rho)f_{\omega\pi\gamma}, \quad (32a)$$

$$F_{\eta\gamma\gamma} = 3^{-1/2}F_{\pi^0\gamma\gamma} \cos\theta[1 - 2\sqrt{2}r \tan\theta]. \quad (32b)$$

From the experimental rates of $\pi^0 \rightarrow 2\gamma$ and $\eta \rightarrow 2\gamma$ we obtain

$$r = 2.71 \pm 0.55 \text{ or } 1.94 \pm 0.55,$$

which are obtained with $\Gamma_{\pi^0 \rightarrow 2\gamma} = 7.74 (1 \pm 0.12)$ eV⁷ or 11.2 ± 1.2 eV,²⁹ respectively. These values with Eqs. (32a) and (32b) lead to

$$f_{\rho\eta\gamma}^2/4\pi = 0.095\alpha \text{ or } 0.108\alpha, \quad (33)$$

respectively. On the other hand, if we use the value of $f_{\omega\pi\gamma}$ determined from the rate $\omega \rightarrow \pi\gamma$, we have

$$f_{\rho\eta\gamma}^2/4\pi = 0.118\alpha \text{ or } 0.092\alpha. \quad (34)$$

The errors associated with (33) and (34) are also about 20%. We see that the agreement between the results in Eqs. (30) and (33) or (34) is very good. This strongly supports our choice of N_0 as the approximate value, which was obtained by following the usual prescription.

To investigate the stability of the result, Eq. (15), we have varied the cutoff N and given an exponential form factor e^{at} to the Regge residue instead of the fixed value given in Eq. (13). In Fig. 3, we plot $\Gamma_{\eta \rightarrow \pi\pi\gamma}$ and $f_{\rho\eta\gamma}^2/4\pi$ as a function of a for both the single-Breit-Wigner and high-low models. We should emphasize that the curves calculated for the single-Breit-Wigner case give the upper limit for the various possible broad-

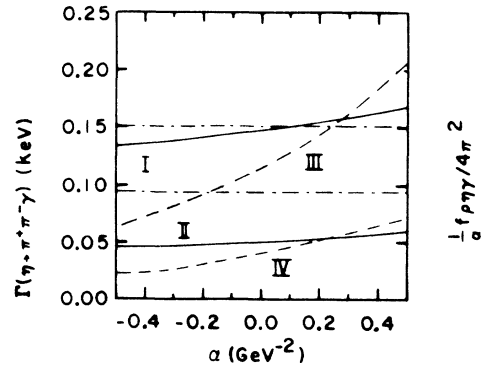


FIG. 3. Plots of predicted values for $\Gamma_{\eta \rightarrow \pi\pi\gamma}$ and $\alpha^{-1}f_{\rho\eta\gamma}^2/4\pi$ as a function of a , where the ρ -Regge residue function or form factor is e^{at} . Curve I: $\Gamma_{\eta \rightarrow \pi\pi\gamma}$ for a single Breit-Wigner resonance (or the upper limit for the broad-narrow picture). Curve II: Upper limit of $\Gamma_{\eta \rightarrow \pi\pi\gamma}$ for the high-low model. Curve III: $\alpha^{-1}f_{\rho\eta\gamma}^2/4\pi$ for a single Breit-Wigner resonance (upper limit for the broad-narrow picture). Curve IV: $\alpha^{-1}f_{\rho\eta\gamma}^2/4\pi$ upper limit value for the high-low model. The horizontal dot-dash lines give the experimental bounds on the rate for $\eta \rightarrow \pi\pi\gamma$ decay.

narrow models, and the curves for the high-low models are upper limits obtaining when couplings to the two narrow resonances to $\pi\eta$ and $\pi\gamma$ are optimal. The curves labeled I and II give $\Gamma_{\eta \rightarrow \pi\pi\gamma}$ vs a , to be read on the left scale, and III and IV give $\alpha^{-1}f_{\rho\eta\gamma}^2/4\pi$ vs a , to be read on the right scale, for the two (single-Breit-Wigner and high-low) cases. The width $\Gamma_{\eta \rightarrow \pi\pi\gamma}$ varies slowly with a , but $f_{\rho\eta\gamma}^2/4\pi$ is rather sensitive to a . The single-Breit-Wigner predictions are within the experimental error bars for zero or small values of a ; thus, one sees that the broad-narrow model can be made to give excellent fits to experiment. However, one sees from Fig. 3 that simultaneous fits within experimental error bars to $\Gamma_{\eta \rightarrow \pi\pi\gamma}$, represented by the dot-dashed lines, and to $f_{\rho\eta\gamma}^2$ are not possible in the high-low picture. Figure 4 shows plots of these same two quantities as a function of N_0 , the radius of the finite integration contour. The single-Breit-Wigner model, and therefore the broad-narrow model, again give good results, although slightly higher values of N_0 will improve them. The high-low model can give acceptable predictions only at the expense of reducing N_0 considerably, i.e., $N_0 \leq 2.0 \text{ GeV}^2$.

We have also investigated the effect of the trajectory functions. If we take the trajectories to have unit slope, instead of the values in Eqs. (11) and (12)

$$\alpha_\rho(t) = 0.415 + t$$

and

$$\alpha_{A_2}(t) = 0.31 + t$$

(giving $m_{A_2}^2 = 3.69 \text{ GeV}^2$), the radius of finite contour becomes $N_0 = 2.5 \text{ GeV}^2$. Repeating the calculation, we obtain

$$\Gamma'_{\eta \rightarrow \pi\pi\gamma} = \begin{cases} 0.16 \text{ keV} & \text{for a single-Breit-Wigner model} \\ 0.056 \text{ keV} & \text{for the high-low model.} \end{cases}$$

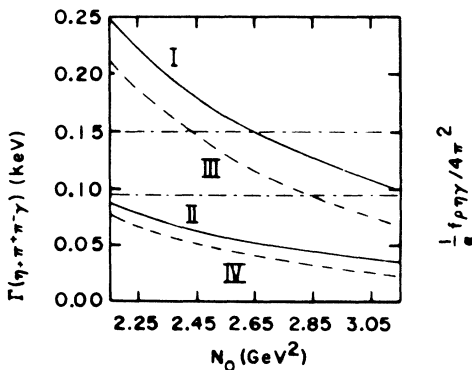


FIG. 4. Plots of $\Gamma_{\eta \rightarrow \pi\pi\gamma}$ and $\alpha^{-1}f_{\rho\eta\gamma}^2/4\pi$ as a function of N_0 . The notation given in the caption of Fig. 3 applies.

Again errors of about 20% are attached to the above values. The single-Breit-Wigner model or any model with a wide component is still favored.

V. CONCLUSION

The method of combining finite dispersion relations and finite energy sum rules appears to be a useful way of predicting three-body decay rates from known couplings and Regge-pole exchanges. In $\eta\pi \rightarrow \gamma\pi$ both ρ exchange in the t channel and A_2 exchange in the s and u channels are required; neither pole by itself saturates the width of $\eta \rightarrow \pi\pi\gamma$. Perfectly satisfactory agreement between calculation and experiment for $\Gamma(\eta \rightarrow \pi\pi\gamma)$ on one hand and between calculation and the broken-SU(3) prediction on the other are found with the A_2 as a single-pole resonance. This calculation, however, does not discriminate between a single-Breit-Wigner model or the two-pole models with a broad resonance (e.g., broad and narrow mixed or interfering resonances of the double-pole model in Refs. 25 and 26). But, within the framework of the present calculation and within the assumptions herein, the A_2 meson as a single, 85-MeV-width resonance leads to a parameter-free prediction of the $\eta \rightarrow \pi^+\pi^-\gamma$ decay rate which is in fine agreement with experiment. We feel that this is rather strong support for the position taken by Bowen *et al.*¹⁵ On the other hand, with a wide and narrow system of two resonances, the calculated value for the decay rate of $\eta \rightarrow \pi\pi\gamma$ can be easily brought into agreement with measurement if the couplings of the two mesons to $\eta\pi$ and $\pi\gamma$ are chosen with the broad resonance dominating in both channels. However, the case with the broad resonance coupling to one channel and with the narrow resonance dominating the coupling to the other channel (in either a mixed or interfering situation) is strongly ruled out.

Regardless of parameter adjustments, models with narrow, separate resonances fail to satisfy or saturate the width relations, yielding predictions for widths and couplings well below experimental limits. Therefore, we feel that the numerous versions of the high-low model^{11,12,14} are unreasonable descriptions of the A_2 meson and should not be included in future particle data tabulations (see, e.g., Ref. 7).

Our results were shown in Sec. IV to be stable to reasonable variations in N_0 , the contour integral radius, and to variation of the Regge form factor. We feel from this and the earlier brief report of the results³⁰ that one may safely say that the A_2 , whether a compound system or not, has a broad, ~ 85 -MeV-width resonance in it which

produces the lion's share of the coupling to $\pi\eta$ and $\pi\rho$ states. This is consistent with the usual phenomenological treatment of the A_2 as a single broad object in, e.g., many t -channel Regge-pole-exchange models.

ACKNOWLEDGMENTS

The authors would like to acknowledge useful conversations with several of their colleagues at Iowa State University and the National Accelerator

Laboratory. Particularly, B.-L. Young and K. E. Lassila are grateful to Professor S. Treiman and Professor J. D. Jackson, respectively, for their hospitality during their visits at NAL. The first author would also like to thank Dr. J. Uretsky for his hospitality during a summer visit to the Argonne Laboratory. The second author acknowledges support through the Faculty Improvement Leave program of Iowa State University during his NAL visit.

*Operated by Universities Research Association Inc. under contract with the U. S. Atomic Energy Commission.

¹S. Nussinov and J. L. Rosner, Phys. Rev. Letters **23**, 1264 (1969).

²K. Kawarabayashi and S. Kitakado, Phys. Rev. Letters **23**, 440 (1969).

³R. Aviv and S. Nussinov, Phys. Rev. D **2**, 209 (1970).

⁴M. Gell-Mann, D. Sharp, and W. Wagner, Phys. Rev. Letters **8**, 261 (1962).

⁵R. Dolen, D. Horn, and C. Schmid, Phys. Rev. **166**, 1768 (1968); K. Igi and S. Matsuda, Phys. Rev. Letters **18**, 625 (1967); **18**, 822 (1967).

⁶G. J. Gounaris and A. Verganelaski, Nucl. Phys. **B34**, 418 (1971).

⁷Particle Data Group, Rev. Mod. Phys. **43**, S1 (1971).

⁸R. J. N. Phillips, in *High Energy Physics*, edited by P. Urban (Springer, New York, 1970); V. Barger and R. J. N. Phillips, Phys. Letters **31B**, 643 (1970).

⁹J. Baacke and J. Engels, Nucl. Phys. **B51**, 434 (1973).

¹⁰J. Ellis and P. H. Weisz, Nuovo Cimento **4A**, 873 (1971); G. Gounaris, Phys. Letters **41B**, 329 (1972).

¹¹D. J. Crennell, U. Karshon, K. W. Lai, J. S. O'Neall, and J. M. Scarr, Phys. Rev. Letters **22**, 1327 (1969).

¹²M. Gell-Mann and G. Zweig, paper presented by G. Zweig, in *Proceedings of the Fourteenth International Conference on High Energy Physics, Vienna, 1968*, edited by J. Prentki and J. Steinberger (CERN, Geneva, Switzerland, 1968). A summary of this work along with predictions are included in a rapporteur's talk by H. Harari in the same proceedings (see p. 197).

¹³The reader may refer to the paper by Aviv and Nussinov, Ref. 1, for details of our procedure in the use of FESR at $t=0$.

¹⁴G. Chikovani *et al.*, Phys. Letters **25B**, 44 (1967).

¹⁵D. Bowen *et al.*, Phys. Rev. Letters **26**, 1663 (1971).

¹⁶J. Rosner, Bull. Am. Phys. Soc. **16**, 610 (1971).

¹⁷K. W. Lai, in *Phenomenology in Particle Physics* (California Institute of Technology, Pasadena, California, 1971), p. 257.

¹⁸M. Alston-Garnjost *et al.*, Phys. Letters **34B**, 156 (1971).

¹⁹J. Lefrancois, in *Proceedings of the International*

Symposium on Electron and Photon Interactions at High Energies, 1971, edited by N. B. Mistry (Cornell Univ. Press, Ithaca, New York, 1972), p. 51.

²⁰The width of $A_2^+ \rightarrow \pi^+\gamma$ has been estimated to be 0.5 MeV by Y. Eisenberg *et al.* [Phys. Rev. Letters **22**, 1322 (1969)] from data on photoproduction, $\gamma + p \rightarrow n + A_2^+$.

²¹For an over-all fit of various meson decay widths in the Gell-Mann-Sharp-Wagner model, including $\eta \rightarrow \pi\pi\gamma$, see A. Baracca and A. Bramon, Nuovo Cimento **69A**, 613 (1970).

²²This value is calculated from information given in Ref. 7.

²³A. M. Cnops, G. Finocchiaro, P. Mittner, P. Zanella, J. P. Dufey, B. Gobbi, M. A. Pouchon, and A. Müller, Phys. Letters **26B**, 398 (1968).

²⁴K. E. Lassila and P. V. Ruuskanen, Phys. Rev. Letters **19**, 762 (1967). A more general discussion with relativistic parametrization is given in Ref. 25. Other later investigations emphasizing various aspects of particle mixing in the A_2 region are: Y. Fujii and M. Kato, Phys. Rev. **188**, 2319 (1969); T. J. Gajdicar and J. Moffat, *ibid.* **181**, 1875 (1969); R. C. Arnold and J. Uretsky, Phys. Rev. Letters **23**, 444 (1969); J. V. Beaupré, T. P. Coleman, K. E. Lassila, and P. V. Ruuskanen, *ibid.* **21**, 1849 (1968).

²⁵P. V. Ruuskanen and K. E. Lassila, in *Proceedings of the Third Topical Conference on Resonant Particles*, Athens, Ohio, 1967 (unpublished).

²⁶Since the basis for the intermediate particles is arbitrary, $a^\dagger a = 1$ (where a performs a unitary transformation on the basis states) can be inserted between each of the factors in Eq. (17). Unitarity requirements on T then lead to a bound on the off-diagonal elements.

²⁷R. H. Dalitz, in *Physical Problems in Biological Systems*, edited by Cécile DeWitt (Gordon and Breach, New York, 1970), p. 253.

²⁸ $f_{\omega\pi\gamma}$ is dimensionless and is defined by

$$\langle \pi, q | j_\mu^{\text{em}}(0) | \omega, p, \epsilon \rangle = m_\pi^{-1} f_{\omega\pi\gamma} \epsilon_{\mu\nu\lambda\rho} \epsilon^\nu(p) q^\lambda p^\rho.$$

²⁹G. Belletini *et al.*, Nuovo Cimento **66A**, 243 (1969).

³⁰K. E. Lassila and B.-L. Young, Phys. Rev. Letters **28**, 1491 (1972).